



Functional activity and morphology of isolated rat cardiac mitochondria under calcium overload. Effect of naringin

T. A. Kavalenia¹ · E. A. Lapshina¹ · T. V. Ilyich¹ · Hu-Cheng Zhao² · I. B. Zavodnik¹

Received: 19 July 2023 / Accepted: 8 January 2024

© The Author(s), under exclusive licence to Springer Science+Business Media, LLC, part of Springer Nature 2024

Abstract

The function of mitochondria as a regulator of myocyte calcium homeostasis has been extensively discussed. The aim of the present work was further clarification of the details of modulation of the functional activity of rat cardiac mitochondria by exogenous Ca^{2+} ions either in the absence or in the presence of the plant flavonoid naringin. Low free Ca^{2+} concentrations (40–250 nM) effectively inhibited the respiratory activity of heart mitochondria, remaining unaffected the efficacy of oxygen consumption. In the presence of high exogenous Ca^{2+} ion concentrations (Ca^{2+} free was 550 μM), we observed a dramatic increase in mitochondrial heterogeneity in size and electron density, which was related to calcium-induced opening of the mitochondrial permeability transition pores (MPTP) and membrane depolarization (Ca^{2+} free ions were from 150 to 750 μM). Naringin partially prevented Ca^{2+} -induced cardiac mitochondrial morphological transformations (200 μM) and dose-dependently inhibited the respiratory activity of mitochondria (10–75 μM) in the absence or in the presence of calcium ions. Our data suggest that naringin (75 μM) promoted membrane potential dissipation, diminishing the potential-dependent accumulation of calcium ions by mitochondria and inhibiting calcium-induced MPTP formation. The modulating effect of the flavonoid on Ca^{2+} -induced mitochondria alterations may be attributed to the weak-acidic nature of the flavonoid and its protonophoric/ionophoric properties. Our results show that the sensitivity of rat heart mitochondria to Ca^{2+} ions was much lower in the case of MPTP opening and much higher in the case of respiration inhibition as compared to liver mitochondria.

Keywords Cardiac mitochondria · Calcium · Ultrastructure · Respiration · Naringin

Abbreviations

ADP	adenosine 5'-diphosphate sodium salt
ANT	adenine nucleotide translocase
BKA	bongkrekate
BSA	bovine serum albumin
CsA	cyclosporine A
EDTA	ethylenediaminetetraacetic acid disodium salt
EGTA	ethylene glycol-bis(β -aminoethyl ether)- N,N,N',N'-tetraacetic acid tetrasodium salt
ER/SR	endoplasmic/sarcoplasmic reticulum
FCCP	carbonyl cyanide 4-(trifluoromethoxy) phenylhydrazone

HEPES	4-(2-Hydroxyethyl)piperazine-1-ethanesulfonic acid
IFM	interfibrillar mitochondria
Me	median, MCU - mitochondrial Ca^{2+} uniporter
MPTP	mitochondrial permeability transition pores
PBS	isotonic buffered saline
RCR	respiratory control ratio
ROS	reactive oxygen species
RuR	Ruthenium red
SERCA	sarcoplasmic reticulum Ca^{2+} -ATPase
SSM	subsarcolemmal mitochondria

✉ I. B. Zavodnik
zavodnik_il@mail.ru; zavodnik_ib@grsu.by

¹ Department of Biochemistry, Yanka Kupala State University of Grodno, Bulvar Leninskogo Komsomola, 5, 230009 Grodno, Belarus

² Institute of Biomechanics and Medical Engineering, Tsinghua University, Beijing 100084, People's Republic of China

Introduction

The never resting heart is a highly active organ that produces an extraordinary amount of work, requires a high rate of energy flux and a constant supply of metabolic substrates, consumes 10% of the body's total oxygen uptake and makes 35 kg of ATP every day during mitochondrial oxidative phosphorylation [1]. Mitochondria occupy roughly 33%

of the cellular volume in each ventricular myocyte [2, 3]. This is the largest mitochondrial volume-fraction found in any mammalian cell. To produce energy, the heart muscle mitochondria is known to consume different substrates, fatty acids, glucose, amino acids, pyruvate, lactate, ketone bodies, and even its own constituent proteins. Cardiac mitochondria structural integrity and appropriate functioning are important for normal heart physiology and perturbations in the ability of heart to produce energy or to consume the substrates results in myocardial dysfunctions and cardiovascular disease [1, 4–6].

The steady-state mitochondrial Ca^{2+} ($[\text{Ca}^{2+}]_m$) level is a key regulator of myocardial energy metabolism, O_2 consumption, proton motive force generation, and ATP production through enhancements in the activities of several mitochondrial substrate transporters and dehydrogenases (Krebs cycle enzymes, an electron transport chain, and F1F0 ATP-synthase) in myocytes, gene expression and cardiomyocyte growth [6, 7].

The role of calcium-dependent processes in cardiac physiology and pathophysiology and, vice versa, the function of mitochondria as a Ca^{2+} buffer and a regulator of calcium homeostasis in cardiac cells have been widely discussed. Impairments in $[\text{Ca}^{2+}]_m$ cycling and mitochondrial network imbalance result in disorders of cellular metabolism and signaling and are the cause of numerous diseases: stroke, heart failure, neurodegeneration, diabetes, and cancer [8–11].

Induction of the mitochondrial permeability transition pore (MPTP, a high-conductance channel) by Ca^{2+} ions overload and reactive oxygen species (ROS) accumulation can provoke loss of mitochondrial membrane potential and subsequent loss of mitochondrial Ca^{2+} . As shown in the earlier work, this transient opening of the MPTP participates in the development of spontaneous contractions and subsequent ventricular arrhythmia [12].

The molecular machinery that mediates calcium flux across the inner mitochondrial membrane includes a highly selective Ruthenium red (RuR)-sensitive mitochondrial Ca^{2+} uniporter complex (consisting of MCU, EMRE, MICU1, MICU2, MICU3, MCUB, and MCUR1 proteins), the mitochondrial $\text{Na}^+/\text{Ca}^{2+}$ exchanger (NCLX), the mitochondrial $\text{H}^+/\text{Ca}^{2+}$ exchanger (Letm1), the mitochondrial ryanodine receptor, and the MPTP [10, 13, 14]. It should be noted that in excitable cells, mitochondria are localized in the vicinity of voltage operated plasma membrane Ca^{2+} channels and can buffer entering Ca^{2+} ions [15].

Effective heart failure pharmacological therapies appear to lead to mitochondrial dysfunction improvement, regulation of cardiomyocyte calcium homeostasis and prevention of mitochondrial ROS generation [16, 17]. The increasing number of results support the beneficial cardioprotective, anti-inflammatory, hypoglycemic, and antioxidant effects of

naringin (4',5,7-trihydroxyflavanone-7-rhamnoglucoside), a bioflavonoid that is abundant in citrus species [18, 19]. However, the detailed mechanisms of the cardioprotective effects of naringin are not fully understood. Recently it was shown that naringin exerts cardioprotection through multiple mechanisms: reducing diastolic $[\text{Ca}^{2+}]$ overload, improving cardiomyocyte glucose uptake, restoring the activities of mitochondrial tricarboxylic acid cycle and respiratory chain enzymes, decreasing ROS production, reducing the level of myocardial tumor necrosis factor- α and interleukin-6 and the expression of NF- κ B [18, 19]. In our previous experiments with rat liver mitochondria, we showed stimulation of calcium-induced MPTP formation by the flavonoids naringenin, catechin, and naringin and hypothesized that the effect of the flavonoids on MPTP opening could be mediated by stimulation of the Ca^{2+} uniporter [20].

Despite numerous investigations, the mechanism(s) of modulation of mitochondrial and cellular functions in cardiac muscles by Ca^{2+} remain unclear. In the present work, we further assessed the details of regulation of MPTP sensitivity, respiratory activity and morphology of isolated rat heart mitochondria by different concentrations of exogenous Ca^{2+} ions. Simultaneously, we estimated the efficiency of correction of Ca^{2+} -induced cardiac mitochondria alterations by the polyphenol naringin (flavanone-7-*O*-glycoside). Understanding the mechanisms of inhibition of the MPTP opening may be useful for the treatment of diseases associated with MPTP that is responsible for tissue damage under stroke and heart attack. Better knowledge of the mitochondria-related influence of polyphenols is important for the design of safe naringin-based nutraceuticals.

Materials and methods

Chemicals

Calcium chloride dehydrate, succinic acid disodium salt hexahydrate, sucrose, ethylene glycol-bis(β -aminoethyl ether)-N,N,N',N'-tetraacetic acid tetrasodium salt (EGTA), carbonyl cyanide *p*-trifluoromethoxyphenyl hydrazone (FCCP), bovine serum albumin fraction V (BSA), ethylenediamine-tetraacetic acid disodium salt (EDTA), 4-(2-Hydroxyethyl) piperazine-1-ethanesulfonic acid (HEPES), Araldite 506 Epoxy resin, adenosine 5'-diphosphate sodium salt (ADP), cyclosporin A (CsA), lead citrate, uranyl acetate, Ruthenium red (RuR), naringin (4',5,7-Trihydroxy-flavanone 7-rhamnoglucoside) (71,162), ethanol, and other chemicals were purchased from Merck / Sigma-Aldrich (St Louis, MO, USA, or Steinheim am Albuch, Germany). Osmium tetroxide suitable for electron microscopy was purchased from Carl Roth GmbH (Karlsruhe, Germany). All solutions were made with water purified in the Milli-Q Direct system (Merck KGaA,

Darmstadt, Germany). Organic solvents were of analytical grade and used without further purification.

Free calcium concentrations. To determine the effects of calcium ions on mitochondrial functions in the presence of EGTA, the added $[Ca^{2+}]_{free}$ for a given $[Ca^{2+}]_{total}$ was determined using Ca-EGTA online calculator [21].

Isolation of rat heart mitochondria

Male albino Wistar rats (200–230 g) were used. The care, use, and all procedures performed were approved by the Ethic Committee of the Institute of Biochemistry of Biologically Active Compounds of the National Academy of Sciences of Belarus (Protocol No 29/20 of 23.05.2020) and complied with the European Convention for the Protection of Vertebrate Animals Used for Experimental and Other Scientific Purposes and the *Guide for the Care and Use of Laboratory Animals* [22].

The coupled myocardium mitochondria were isolated from the rat heart by the method of differential centrifugation [7, 23, 24]. We used the isolation medium containing 0.25 M sucrose, 0.005 M HEPES, 0.0002 M EDTA, and 0.1% BSA, pH 7.4. The isolated heart was quickly transferred into an ice-cold 0.9% KCl solution and carefully washed from the blood. The muscle tissue was weighed, crushed with scissors on ice and homogenized using a glass homogenizer with a Teflon pestle in the isolation medium at 4 °C. The nuclear fraction was removed by centrifugation at 650 g (10 min, 4 °C) (a Hermle Z 32 HK centrifuge, Hermle Labortechnik GmbH, Germany). The mitochondria were sedimented by centrifugation at 8 500 g (10 min, 4 °C) and washed two times with the isolation medium. The pellet of mitochondria was resuspended to an approximate protein concentration of 25–30 mg/ml in the isolation medium. Protein concentrations in myocardium mitochondria were determined by the method of Lowry et al. [25].

Electron microscopy of isolated rat heart mitochondria

Rat cardiac muscle mitochondria (5 mg/ml) were exposed to Ca^{2+} ions (550 μ M free Ca^{2+}), the flavonoid naringin (200 μ M) or Ca^{2+} ions (550 μ M free Ca^{2+}) plus the flavonoid naringin (200 μ M) in the medium containing 0.25 M sucrose, 0.005 M HEPES, 0.005 M KH_2PO_4 and 0.00005 M EGTA, pH 7.4, for 30 min (26 °C) *in vitro*. After calcium and flavonoid exposure, the suspensions of mitochondria were centrifuged at 10 000 g and +4 °C for 20 min. Then the mitochondrial pellets were fixed by 2.5% glutaric aldehyde and postfixed in two portions of 1% osmium tetroxide solution in 0.1 M Millonig buffer, pH 7.4 at +4 °C for 2 h [26].

After dehydration by rinsing in alcohols of increasing concentrations and acetone, the samples were embedded in

Araldite Epoxy resin. The sections were prepared using a Leica EM UC7 ultramicrotome (Leica Microsystems GmbH, Germany). Semi-thin sections were stained with a 1% solution of methylene blue, whereas ultrathin (35 nm) sections were contrasted with a 2% solution of uranyl acetate and lead citrate by the method of Reynolds [27] and analyzed with a JEM-1011 electron microscope (Japanese Electron Optics Laboratory Ltd., Japan) at magnifications of 5 000–40 000 and accelerating voltage of 80 kilowatts. Images were captured with an Olympus Mega View III digital camera (Olympus Corporation, Germany). The digital images were used to determine some ultrastructural parameters characterizing the structure, size and shape of these organelles. The morphometric factors were assessed under 20000x or 40000x microscope magnifications on the representative 10 squares (fields of view) tested. Under these magnifications, 250 to 500 mitochondrial profiles were examined. We used 5 animals in each group. For evaluation of the ultrastructural mitochondrial changes, we used such morphometric parameters as Mean Gray value, Area, Elongation factor, Equivalent circle diameter (ECD), Shape factor, Sphericity, Mean Diameter and Aspect ratio, evaluated by the iTEM Olympus Soft Imaging Solutions software (Version 5.0 (Build 1224); Serial Number A3766900-7E852FAB) (Olympus Corporation, Germany), which has a number of standard built-in algorithms for morphometry.

The Mean Gray value is the relative electron density of the mitochondrial matrix (in the iTEM program interface) registered as an average level of Gray of the studied object. The Area (average section area of one mitochondrion) is the average area occupied by the profile of one mitochondrion on a section (μm^2). The Elongation factor assesses the lack of roundness of the object (defined as the ratio of the length to the width of the object); as the “ellipsoidality” increases, this parameter raises above 1. Similarly, the Shape factor characterizes the “roundness” of the object: this parameter is equal to 1 for the spheres, and for all other shapes it is less than 1. The Aspect ratio depends on the ratio of the maximal width and height of the rectangle within which the object is placed. The Equivalent circle diameter (ECD) is the diameter of a circle with an area equivalent to the area of the object measured. The Sphericity assesses the “roundness” of the object measured.

Measurements of mitochondrial respiration and membrane potential

Respiration of cardiac mitochondria was measured using an oxygen Clark-type electrode (Hansatech Instruments Limited, Great Britain) in the medium containing 0.25 M sucrose, 0.005 M KH_2PO_4 , 0.005 M HEPES, 0.01 M KCl, 0.002 M $MgCl_2$, 0.0002 M EGTA, pH 7.4, at 26 °C. The mitochondrial suspension (0.5 mg protein/ml) in

the respiratory buffer was continuously stirred. To study FADH₂-dependent respiration, oxygen consumption rates were determined in the presence of 5 mM succinate as a substrate (respiratory state 2, V₂), after ADP (200 μM) addition (ADP-stimulated state 3, V₃) and after ADP consumption (state 4, V₄). The respiratory control ratio (RCR) equal to the ratio of the respiratory rates (V₃/V₄) of mitochondria in state 3 and state 4 and the coefficient of phosphorylation (ADP/O ratio) were calculated.

Mitochondrial membrane potential was detected using a Perkin-Elmer LS55 Fluorescence Spectrometer (Great Britain) as the changes in the fluorescent intensity of the dye safranin O (8 μM) at λ_{ex}/λ_{em} 495/586 nm [28, 29] in the medium containing 0.25 M sucrose, 0.005 M HEPES, 0.005 M KH₂PO₄, 0.002 M MgCl₂, 0.00005 M EGTA, and 5 mM succinate as a substrate, pH 7.4, at 26 °C. Isolated cardiac mitochondria (0.3 mg of protein/ml) were placed into the media and after 5 min effectors were added. The positively charged dye accumulated in mitochondria depending on the mitochondrial membrane potential, resulting in intramitochondrial dye fluorescence quenching. Complete depolarization of mitochondria to calibrate the dye fluorescence was achieved by addition of the uncoupler FCCP (0.5 μM). The membrane potential changes in the presence of calcium ions or naringin were presented as the ratio (I_{FCCP} - I)/(I_{FCCP} - I₀), where I₀ is initial safranin O fluorescence intensity in mitochondrial suspension, I is safranin O fluorescence intensity, I_{FCCP} is safranin O fluorescence intensity after FCCP addition.

Mitochondrial swelling determination

Ca²⁺-induced swelling of respiring cardiac mitochondria was measured as we described earlier [30]. Briefly, the extent of the mitochondrial permeability transition pore (MPTP) formation was determined from the changes in the optical density of the mitochondrial suspension at 540 nm and 26 °C using the buffer containing 0.12 M KCl, 0.005 M HEPES, 0.005 M KH₂PO₄, 0.002 M MgCl₂, 0.00005 M EGTA, pH 7.4. Isolated mitochondria (0.5 mg of protein/ml) were added to the medium containing respiratory substrate (5 mM succinate). After 5 min of incubation, Ca²⁺ ions or the flavonoid naringin were added and the rate (ΔD⁵⁴⁰/min) of the termination phase of swelling was measured, using a Jasco V-650 UV-VIS Spectrophotometer (Japan). At the end of the measurements, the uncoupler FCCP (0.5 μM) was added to the mitochondria to control the completion of the MPTP formation process. To evaluate the effect of cyclosporine A, an inhibitor of MPTP formation, or RuR, an inhibitor of MCU, the mitochondria were pretreated with 1 μM CsA or 10 μM RuR at 26 °C for 3 min.

Statistics

The data of the experiments, obtained in 5–7 repetitions, were processed statistically by the package of applied program Statistica 10.0 and presented as a median (Me) and an interquartile range between the 25th and the 75th percentile [Q1; Q3]. The normality of distribution was assessed by the Shapiro-Wilk's test. The reliability of differences between the parameters were analyzed using the non-parametric Mann-Whitney U test and the Kruskal-Wallis H test when the data distribution was not the normal distribution and the standard Student t test for the data showing no departures from normality. The level of significance was considered at *P* < 0.05.

Results

Electron microscopic examination of the effects of exogenous Ca²⁺ ions on heart mitochondria ultrastructure

A typical picture of the ultrastructure of mitochondria isolated from the cardiomyocytes of 3-month-old Wistar rats is presented in Fig. 1. The purity of the mitochondrial fraction made up 90–95% in all the samples studied. In the majority of cases there were few admixtures as small fragments of microfibrils and individual lysosomes and lipofuscin granules. Most of the control mitochondria were of a round shape and distinguished by variable sizes (Fig. 1a). Multiple densely packed cristae occupied all the area of the mitochondrion section and the matrix was of moderate electron density. Such organelles are conventionally classified as those preserving orthodox biosynthetic functional state. Some of the mitochondria showed more or less pronounced ultrastructural changes. These organelles were generally distinguished by an irregular shape, a light matrix and a larger size as compared to the majority of the neighboring organelles. It should be noted that control samples displayed only individual mitochondria with pronounced damage.

After exposure to 550 μM free Ca²⁺ ions, we observed appearance of swollen organelles with an electron-light matrix, a larger size, an irregular shape and a damaged native structure of the inner membrane (Fig. 1b). In the setting of the swollen matrix, mitochondria showed the formation of areas completely devoid of cristae, elongation of the intercristae spaces. The cristae which lost contacts with the outer wall were located irregularly and often aggregated on the periphery (Fig. 1b). In this situation, a mitochondrion, with the cristae area being not less than half the total surface area of the section, was classified as the organelle with a moderately disrupted structure, whereas a mitochondrion, with the cristae area being less than half the total square

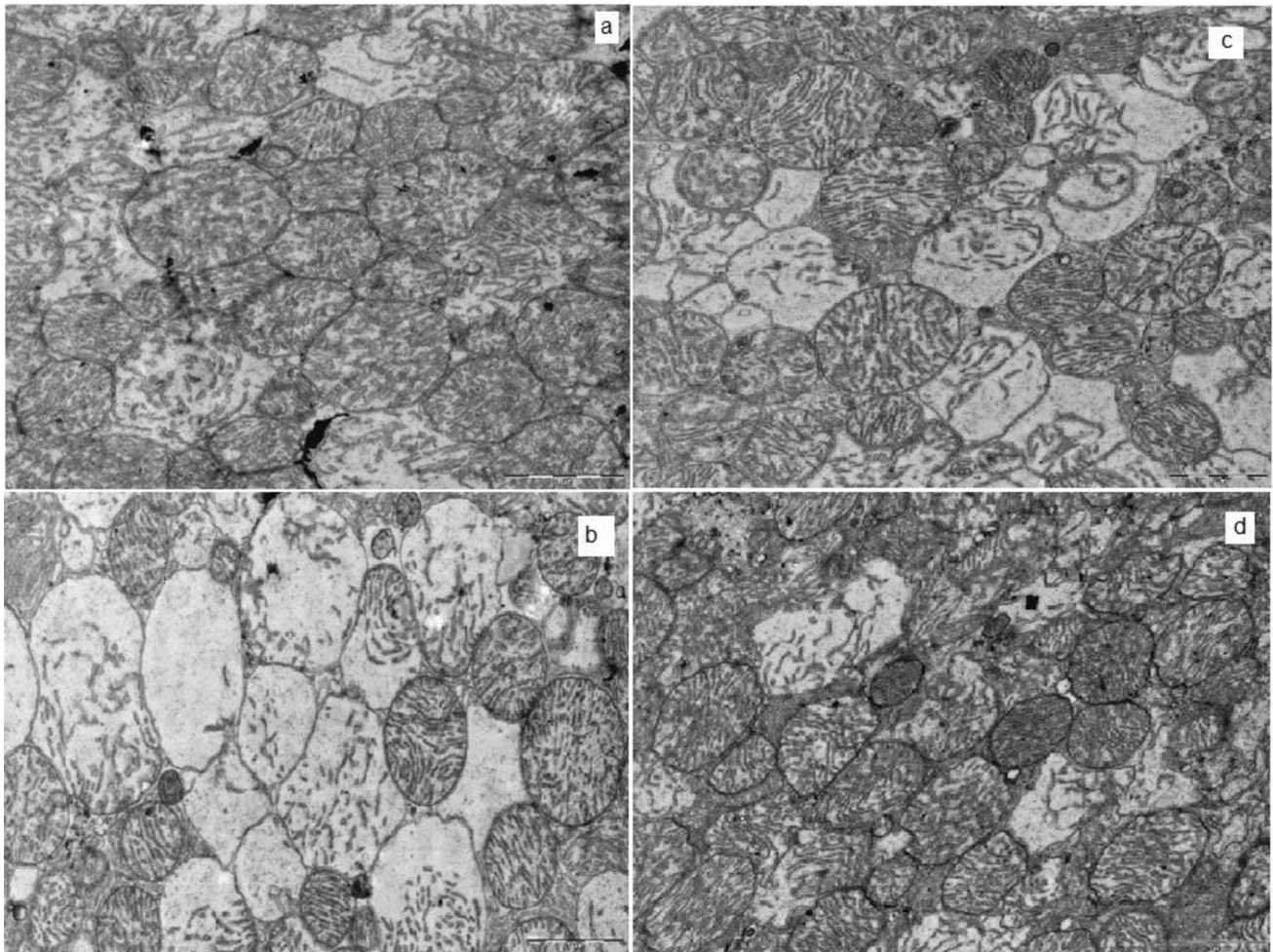


Fig. 1 Electron micrographs of isolated rat heart mitochondria: **a** control rat heart mitochondria, **b** Ca^{2+} -induced morphological transformations of cardiac mitochondria in vitro (Ca^{2+} free = $550 \mu\text{M}$, 30 min, 26°C), **c** heart mitochondria exposed to Ca^{2+} ions ($550 \mu\text{M}$

free Ca^{2+}) in the presence of naringin ($200 \mu\text{M}$, 30 min, 26°C), **d** mitochondria exposed to the flavonoid naringin ($200 \mu\text{M}$, 30 min, 26°C). 0.25 M sucrose, 0.005 M HEPES, 0.005 M KH_2PO_4 , 0.00005 M EGTA, pH 7.4, $\times 40\,000$. The scale intervals are equal to $1.0 \mu\text{m}$

of the section, was classified as the organelle with a substantially impaired structure. Mitochondria with moderately and substantially impaired structures were seen much more frequently in comparison with control. The visual analysis of the ultrastructural transformations was confirmed by morphometrical measurements (Table 1). The mitochondrial exposure to $550 \mu\text{M}$ free Ca^{2+} induced an increase in the cross-section area (by 20%), in the average perimeter (by 12%) and in the mean diameter (by 15%) of one mitochondrion. The elongation factor elevated and the organelle sphericity decreased, with the shape factor remaining changed.

The exposure of heart mitochondria to the flavonoid naringin ($200 \mu\text{M}$) alone induced some visible changes in the organelle ultrastructure (Fig. 1d) and affected the morphometrical parameters: increased the average section area (by 10%), the average perimeter of mitochondria,

the mean diameter and sphericity, but reduced the aspect ratio and elongation factor (Table 1). When mitochondria were exposed to Ca^{2+} ions ($550 \mu\text{M}$ free Ca^{2+}) in the presence of naringin ($200 \mu\text{M}$), we observed prevention of ultrastructural impairments (Fig. 1c, Table 1). The samples of the mitochondrial fraction of this group showed a greater amount of the organelles with preserved structures as opposed to the group exposed to Ca^{2+} without naringin correction and the majority of the organelles were characterized by a round shape, as in the case of control mitochondria, a matrix of moderate electron density and distinct, random cristae. The mean section area, the mean perimeter, and the mean diameter of mitochondria exposure to Ca^{2+} ions in the presence of naringin were not changed in comparison with control organelles (Table 1).

Table 1 Morphometric parameters of isolated rat heart mitochondria before and after treatment by Ca²⁺ ions

Morphometric parameters	Control	550 μM Ca ²⁺ free	550 μM Ca ²⁺ free + naringin 200 μM	Naringin 200 μM
Area (average section area of one mitochondrion), μm ²	0.62 [0.40;0.89]	0.74 [0.44;1.26]*	0.62 [0.39;0.87] [#]	0.67 [0.46;1.01]*
Perimeter (average perimeter of one mitochondrion), μm	3.21 [2.55;3.90]	3.60 [2.78; 4.68]*	3.21 [2.56;3.88] [#]	3.38 [2.76;4.16]*
Aspect ratio	1.48 [1.36;1.62]	1.59 [1.45; 1.76]*	1.57 [1.45;1.73]*	1.42 [1.32;1.59]* [@]
Elongation factor	1.48 [1.34;1.61]	1.57 [1.41; 1.73]*	1.56 [1.45;1.74]*	1.42 [1.29;1.59]* [@]
Mean gray value (mean relative electron density of mitochondria)	115.4 [106.5;131.0]	147.8 [124.8;161.2]*	129.1 [119.4;147.6] [#]	125.1 [108.0;139.3]* [@]
ECD (Equivalent circle diameter), μm	0.89 [0.71;1.07]	0.98 [0.75;1.28]*	0.89 [0.71;1.05] [#]	0.93 [0.76;1.13]* [@]
Mean diameter (average diameter of one mitochondrion), μm	1.01 [0.79;1.22]	1.14 [0.85;1.49]*	1.01 [0.79;1.25] [#]	1.07 [0.88;1.29]* [@]
Sphericity	0.46 [0.38;0.55]	0.41 [0.34;0.50]*	0.42 [0.34;0.49]*	0.52 [0.41;0.61]* [@]
Shape factor	0.78 [0.72;0.82]	0.77 [0.70;0.81]	0.77 [0.71;0.80]	0.78 [0.71;0.82]

Effect of naringin. Rat cardiac muscle mitochondria (5 mg/ml) were exposed to Ca²⁺ ions (550 μM Ca²⁺ free), flavonoid naringin (200 μM) or Ca²⁺ ions (550 μM Ca²⁺ free) plus flavonoid naringin (200 μM) in the medium containing 0.25 M sucrose, 0.005 M HEPES, 0.005 M KH₂PO₄, 0.0005 M EGTA, pH 7.4, for 30 min (26 °C) *in vitro*. We used 5 animals in each group. The results were expressed as Me [Q1; Q3].

* - $p < 0.05$ in comparison with Control

[#] - $p < 0.05$ in comparison with 550 μM Ca²⁺ free

[@] - $p < 0.05$ in comparison with 550 μM Ca²⁺ free + naringin 200 μM

Respiratory parameters of rat heart mitochondria *in vitro* in the presence of Ca²⁺ ions. Effect of plant polyphenol

At the next step of our *in vitro* experiments, we evaluated the effects of Ca²⁺ ions and the flavonoid naringin on the parameters of mitochondrial respiration. The low concentrations of exogenous free Ca²⁺ ions (we used 0.0002 M EGTA-containing medium and the calculated Ca²⁺ free concentrations were from 20 to 250 nM) dose-dependently inhibited the substrate-stimulated oxygen consumption rate V₂ and the ADP-dependent oxygen consumption rate V₃. The coefficient RCR and the coefficient of phosphorylation ADP/O were not considerably changed (Fig. 2a, b). Figure 2c shows representative traces of oxygen consumption by rat heart mitochondria in the absence and in the presence of calcium ions (Online Resource).

Taking into consideration the possibility of plant polyphenols to influence mitochondrial activity, we studied the modulatory effects of the flavonoid naringin, widely distributed in the human diet, on the respiratory parameters of isolated rat cardiac mitochondria in the absence or in the presence of calcium ions (Ca²⁺ free = 240 nM) *in vitro*. In the absence or in the presence of Ca²⁺ ions, naringin (10–75 μM) dose-dependently diminished the ADP-stimulated oxygen-consumption rate V₃ in mitochondria (Fig. 3a). The flavonoid slightly increased oxygen-consumption rate V₂ in the absence of Ca²⁺ and slightly decreased this parameter in the presence of Ca²⁺ (Fig. 3a), as well as decreased the

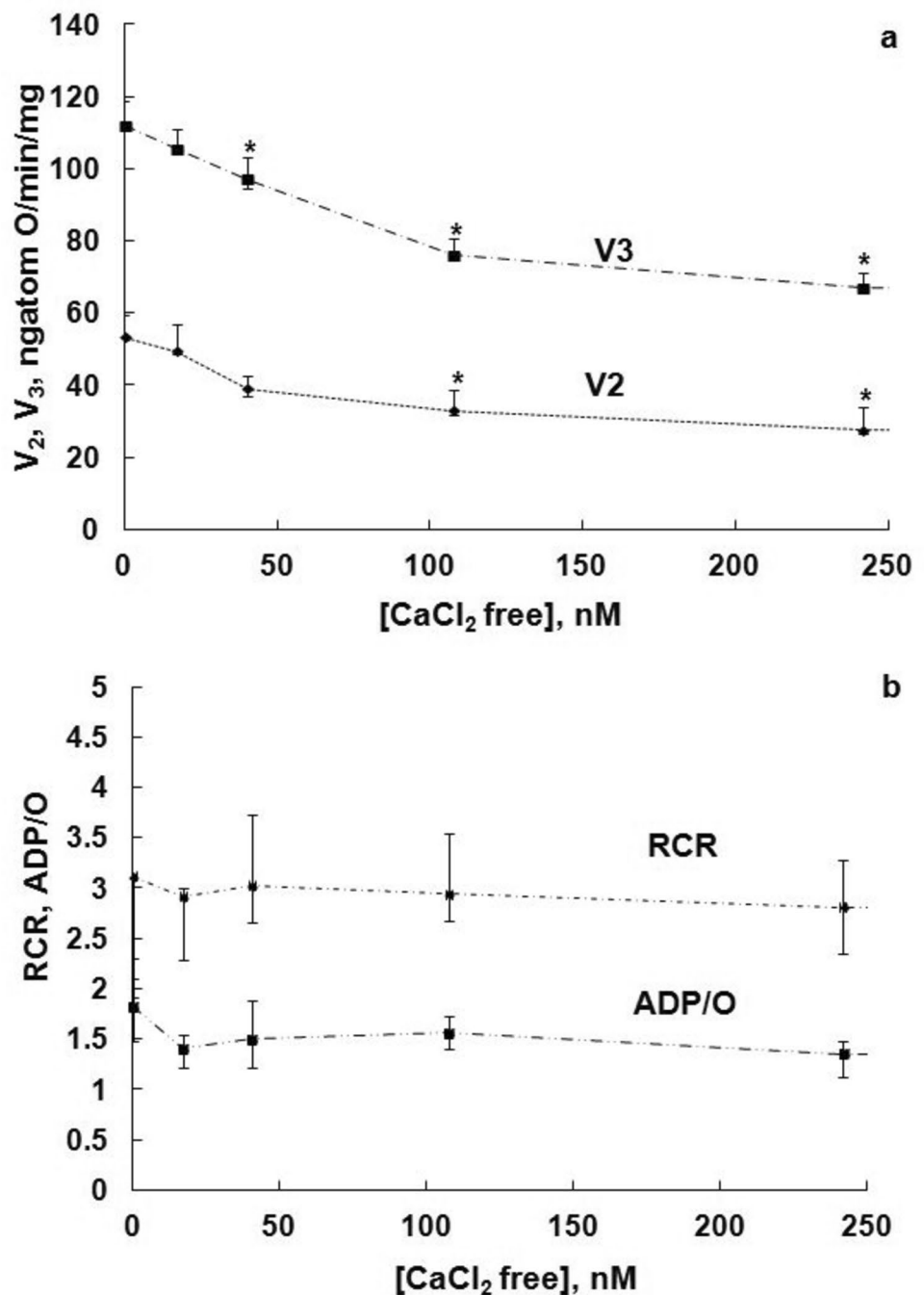
coefficient RCR (V₄/V₃), but did not influence the coefficient ADP/O (Fig. 3b). Figure 3c and d show representative traces of oxygen consumption by rat heart mitochondria in the absence and in the presence of naringin before (Fig. 3c) and after addition (Fig. 3d) of calcium ions (Online Resource).

Heart mitochondria permeability transition and membrane depolarization induced by Ca²⁺ ions and naringin *in vitro*

Further we compared the effects of Ca²⁺ ions on respiratory parameters of cardiac mitochondria with those on swelling and membrane potential of cardiac mitochondria energized by succinate. The rate of MPTP formation was measured using the initial part of the kinetic curves of Ca²⁺-induced mitochondrial swelling. Figure 4a and b show representative tracks of rat heart mitochondrial swelling as a result of MPTP opening that was recorded by changing the intensity of mitochondrial suspension light scattering (D⁵⁴⁰) in the presence of increasing concentrations of Ca²⁺ ions.

As one can see, the apparent rate of MPTP formation dose-dependently increased in the presence of calcium ions (Figs. 4 and 5). CsA, a known inhibitor of MPTP opening, completely prevented heart mitochondria swelling (Fig. 4a). Simultaneously, the higher concentrations of the calcium chelator EGTA (0.0005 M) also prevented Ca²⁺-induced MPTP opening (Fig. 4a). The specific inhibitor of MCU, RuR, completely inhibited Ca²⁺-induced mitochondria

Fig. 2 Ca^{2+} ions inhibit respiratory activity of rat heart mitochondria: dependences of the oxygen consumption rate V_2 , the ADP-dependent oxygen consumption rate V_3 **a**, and the coefficients RCR and ADP/O on Ca^{2+} ion concentrations **b**. Rat heart mitochondria (0.5 mg/ml) were placed in EGTA-containing medium: 0.25 M sucrose, 0.005 M KH_2PO_4 , 0.005 M HEPES, 0.01 M KCl, 0.002 M MgCl_2 , 0.0002 M EGTA, pH 7.4, at 26 °C. 5 mM succinate as a substrate and 200 μM ADP were added. Significant difference ($P < 0.05$): *vs. that in the absence of calcium ions



swelling as well (Fig. 4b). The polyphenolic effector naringin (25–75 μM) promoted mitochondria swelling in the absence of calcium ions (Figs. 4b and 6), but inhibited calcium-induced MPTP formation at higher concentrations (75 μM).

Figure 7a and b show representative traces of the probe safranin O fluorescence intensity changes after exposure of mitochondria to Ca^{2+} ions or naringin. Ca^{2+} ions

($\text{Ca}^{2+}\text{free} = 100\text{--}550 \mu\text{M}$) effectively dissipated mitochondrial membrane potential in the EGTA-containing media. Simultaneously, the heart mitochondria exposure to naringin (75 μM) resulted in dissipation of membrane potential in the absence of Ca^{2+} (Fig. 5). RuR prevented Ca^{2+} -induced dissipation of cardiac mitochondria membrane potential in the absence (completely) or in the presence of naringin (partially) (Fig. 5).

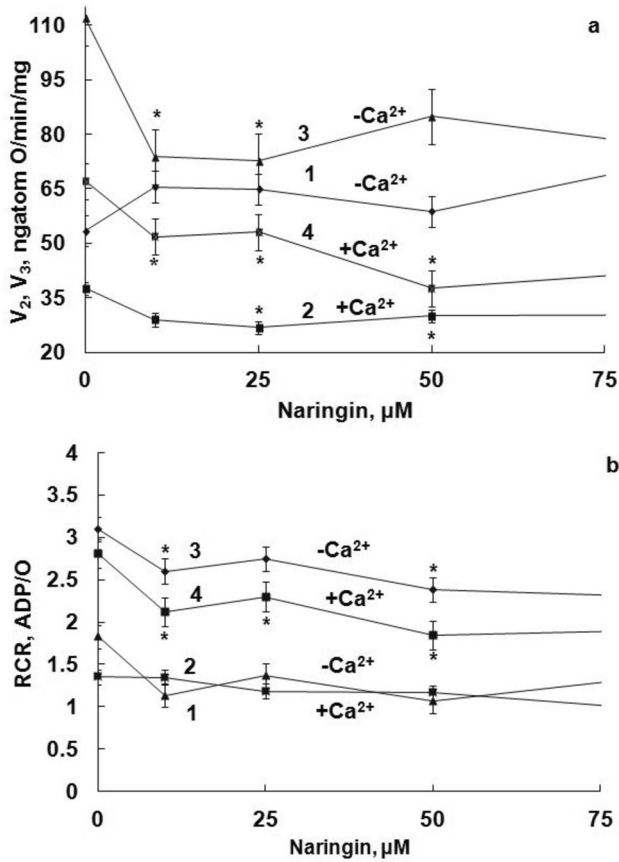


Fig. 3 Effect of naringin on the respiration parameters of isolated rat heart mitochondria: **a** the oxygen consumption rates V₂ (1, 2) and V₃ (3, 4); **b** the coefficient of phosphorylation (ADP/O ratio) (1, 2) and the respiratory control ratio (RCR) (3, 4) in the absence (1, 3) or in the presence of Ca²⁺ ions (Ca²⁺ free = 240 nM) (2, 4). Mitochondria (0.5 mg protein/ml) were placed in the medium containing 0.25 M sucrose, 0.005 M KH₂PO₄, 0.005 M HEPES, 0.01 M KCl, 0.002 M MgCl₂, 0.0002 M EGTA, pH 7.4, at 26 °C, in the absence or in the presence of naringin. 5 mM succinate as a substrate and 200 μM ADP were added. Significant difference (P < 0.05): *vs. that in the absence of naringin

Discussion

Ca²⁺ signaling pathways play fundamental roles in the heart as regulators of the contractile function and cardiomyocyte growth, and altered Ca²⁺ homeostasis is the main cause of cardiovascular diseases [9]. The earlier work of Miyamae et al. showed that cardiac mitochondrial Ca²⁺ was in the range of 0.1–0.2 μM and raised to a higher steady-state level during increasing beating frequency [31]. The cardiomyocyte possesses spatially separated populations of mitochondria which respond to pathological conditions heterogeneously [32]. Subsarcolemmal mitochondria (SSM) exist below the sarcolemma, interfibrillar mitochondria (IFM) reside in the rows between the myofibril contractile apparatus, and perinuclear mitochondria are situated at the nuclear

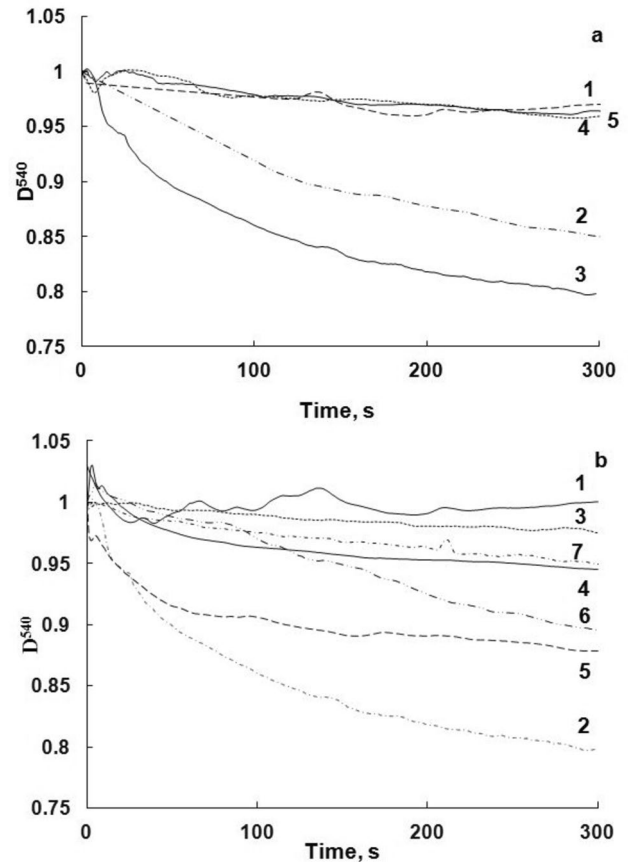


Fig. 4 Representative traces of time-dependences of exogenous Ca²⁺-induced MPTP formations measured as changing optical density (D⁵⁴⁰) of cardiac mitochondrial suspension at 540 nm: **a** in the absence (1, control) and in the presence of exogenous free Ca²⁺ ions: 350 μM (2), 550 μM (600 μM total Ca²⁺ ions) (3), 58 μM (600 μM total Ca²⁺ ions in the presence of 0.0005 M EGTA) (4), 550 μM free Ca²⁺ + 10 μM RuR (5); **b** in the absence (1, control) and in the presence of exogenous free Ca²⁺ ions and naringin: free Ca²⁺ 550 μM (2), free Ca²⁺ 550 μM + 1 μM CsA (3), naringin 25 μM (4), naringin 75 μM (5), free Ca²⁺ 550 μM + naringin 75 μM (6), free Ca²⁺ 550 μM + naringin 75 μM + 10 μM RuR (7). 0.12 M KCl, 0.005 M HEPES, 0.005 M KH₂PO₄, 0.002 M MgCl₂, and 0.00005 M EGTA, pH 7.4 at 26 °C, 5 mM succinate as a substrate, 0.5 mg protein/ml

poles in the perinuclear region [33, 34]. As was shown earlier electron transport chain complex activities do not differ significantly in IFM and SSM [32]. Scanning electron microscopy was used to show that interfibrillar mitochondria were elongated and usually about the same length as the sarcomere and that subsarcolemmal mitochondria varied in size and shape, being rod-like, spherical, polygonal or horseshoe-like [34].

In our experiment, the ultrastructure of the control cardiac rat mitochondria corresponded to the optimal bioenergetic potential. The overload by calcium ions (free Ca²⁺ concentration was 550 μM) demonstrated a dramatic increase in mitochondrial heterogeneity in size and electron density,

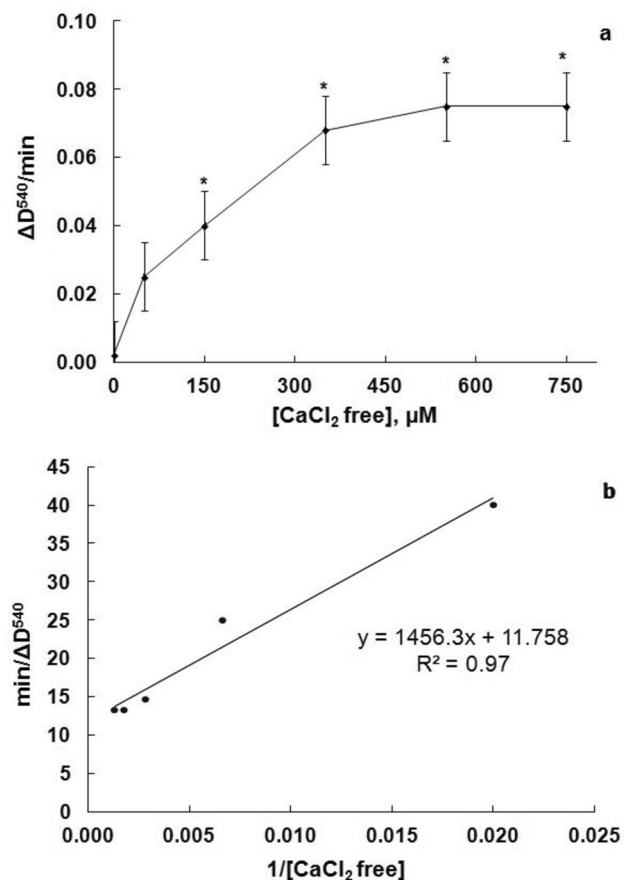


Fig. 5 Effect of free Ca^{2+} ion concentrations on the rate of MPTP ($\Delta\text{D}^{540}/\text{min}$) formation for rat heart mitochondria (a), the same dependence represented as the Lineweaver-Burk plot (or a double reciprocal plot) (b). 0.12 M KCl, 0.005 M HEPES, 0.005 M KH_2PO_4 , 0.002 M MgCl_2 , and 0.00005 M EGTA, pH 7.4 at 26 °C, 5 mM succinate as a substrate, 0.5 mg protein/ml. Significant difference ($P < 0.05$): *vs. that in the absence of Ca^{2+} ions

resulting in swelling mitochondria which were characterized by lowered bioenergetic and biosynthetic potentials.

Our present findings add new insight into the mitochondria-related effects of polyphenols and the mechanisms underlying the modulation by naringin of calcium-induced mitochondrial permeability transition pore formation and membrane depolarization. We demonstrated an influence of naringin alone on the isolated heart mitochondria ultrastructure. In our work, naringin influenced mitochondrial functions and affected the response of rat heart mitochondria to Ca^{2+} ions: the preliminary exposure of the mitochondria to naringin partially prevented Ca^{2+} ion-induced structural transformations, naringin dose-dependently inhibited mitochondrial oxygen consumption, stimulated MPTP opening and membrane depolarization in the absence of Ca^{2+} (this fact correlated with the morphological transformations of mitochondria observed in the presence of naringin), but partially prevented Ca^{2+} -induced MPTP opening (25–100

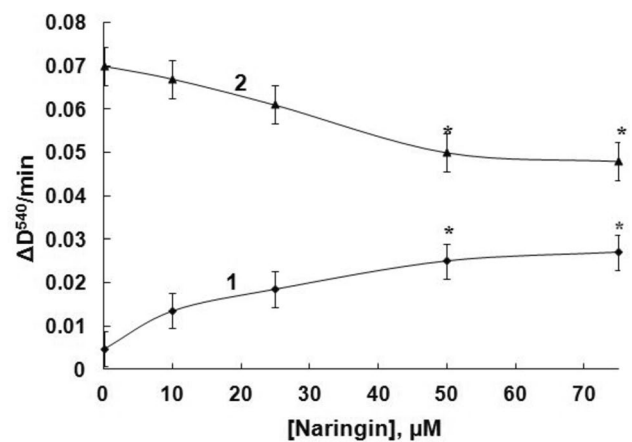


Fig. 6 Effect of naringin on the rate of MPTP ($\Delta\text{D}^{540}/\text{min}$) formation for rat heart mitochondria in the absence (1) and in the presence of free Ca^{2+} 550 mM (2). 0.12 M KCl, 0.005 M HEPES, 0.005 M KH_2PO_4 , 0.002 M MgCl_2 , and 0.00005 M EGTA, pH 7.4 at 26 °C, 5 mM succinate as a substrate, 0.5 mg protein/ml. Significant difference ($P < 0.05$): *vs. that in the absence of naringin

μM). The decrease in membrane potential by naringin probably diminished potential-dependent calcium ion accumulation by mitochondria. In our experiment, RuR, a specific inhibitor of the mitochondrial calcium uniporter, completely inhibited Ca^{2+} -dependent membrane depolarization, but did not affect markedly the stimulation of these processes by naringin. The uncoupling effect of the flavonoids and their ability to dissipate mitochondrial membrane potential have been attributed to weak-acidic and hydrophobic nature of the flavonoids [35].

For rat liver mitochondria we previously suggested a direct incorporation of the flavonoids, quercetin, catechin and naringenin, in the mitochondrial membrane and a change in membrane stability, as well as an effect of the flavonoids as proton/calcium ions carriers and Ca^{2+} ions chelators [36]. It is well-known that a large number of plant flavonoids are capable of forming stable metal complexes through their multiple OH groups and the carbonyl moiety and of preventing the toxicity of active metal ions [37]. The reactive polyphenols can act as either agonists or antagonists of MPTP opening depending on the experimental conditions and polyphenol concentrations [38, 39]. One of the main results of the mitochondrial calcium overload is the MPTP formation resulting in Ca^{2+} linked necrotic and apoptotic (or necroapoptotic) myocyte death [40]. We suggested that the Ca^{2+} -induced ultrastructural disturbances in rat heart mitochondria and mitochondrial membrane depolarization were probably a result of MPTP opening (free Ca^{2+} concentrations were 150–750 μM) (Fig. 5) and that the changes in the mitochondrial respiratory activity were not related to the MPTP formation. The molecular mechanisms of MPTP formation remain rather controversial. Using mouse embryonic

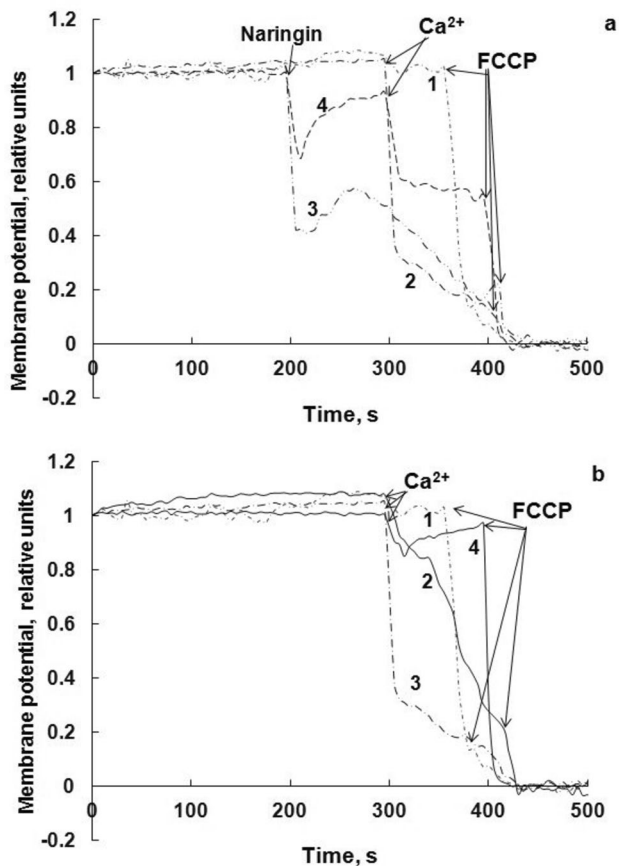


Fig. 7 Representative traces of rat heart mitochondrial membrane potential dissipation: **a** control (1); 550 μM Ca^{2+} (2); 75 μM naringin (3); 550 μM Ca^{2+} + 75 μM naringin + 10 μM RuR (4); **b** control (1); 100 μM Ca^{2+} (2); 550 μM Ca^{2+} (3); 550 μM Ca^{2+} + 10 μM RuR (4). Mitochondrial membrane potential was detected using the fluorescent dye safranin O (8 μM) at $\lambda_{\text{ex}}/\lambda_{\text{em}}$ 495/586 nm, at 27 $^{\circ}\text{C}$ and 5 mM succinate as energizing substrate. Mitochondria (0.3 mg of protein/ml) were added to the medium at constant gentle stirring: 0.25 M sucrose, 0.005 M HEPES, 0.005 M KH_2PO_4 , 0.002 M MgCl_2 , 0.00005 M EGTA, and 5 mM succinate as a substrate, pH 7.4, at 26 $^{\circ}\text{C}$

fibroblasts, it has been shown recently that Ca^{2+} -induced CsA-sensitive depolarization preceded opening of high-conductance MPTP, which occurred only after nearly complete mitochondrial membrane depolarization (defined as low-conductance permeability transition) [41].

Using the Lineweaver-Burk plot of the dependence of the reciprocal apparent swelling rate ($\text{min}/\Delta\text{D}^{540}$) on the reciprocal Ca^{2+} concentration ($1/[\text{Ca}^{2+}]$), we calculated the apparent Michaelis-Menten constant, K_m , of Ca^{2+} ions interaction with rat cardiac mitochondria sites (or Ca^{2+} concentration corresponding to half the maximal swelling rate) (Fig. 5b). The apparent K_m of the MPTP formation for cardiac mitochondria was calculated to be $350 \pm 50 \mu\text{M}$. Earlier it was shown that the cardiac MCU conductance was assumed to follow a Michaelis-Menten type relationship with a K_m of

19 mM Ca^{2+} and that MCU flux appeared to be modulated by $[\text{Ca}^{2+}]_i$ [42]. For comparison, the apparent K_m for MPTP formation in the isolated rat liver mitochondria was previously calculated to be $75 \pm 20 \mu\text{M}$ [30]. Bernardi has recently suggested at least two pathways for Ca^{2+} -dependent mitochondria permeabilization: (1) high-conductance F-ATP synthase-dependent MPTP opening, which is inhibited by CsA, but not by bongkrekate (BKA), and (2) adenine nucleotide translocase (ANT) dependent MPTP opening, which is inhibited by both CsA and BKA [43]. Halestrap et al. suggested the MPTP to be a promising drug target in human cardiovascular disease [44].

According to our results, low free Ca^{2+} concentrations (40–250 nM) effectively inhibited the respiratory activity of rat heart mitochondria, remaining unaffected the coefficient ADP/O. Inhibition of the respiratory activity of heart mitochondria preceded Ca^{2+} -linked MPTP or membrane depolarization.

Biphasic Ca^{2+} effects such as small increases in Ca^{2+} concentration stimulating mitochondrial respiration and considerable Ca^{2+} elevations inhibiting respiration were detected both in heart and kidney mitochondria [7, 45]. The sensitivity of O_2 utilization and ATP synthesis to Ca^{2+} ions were substrate-dependent and organ (heart and kidney) – specific [7]. Similarly, using isolated mice skeletal muscle mitochondria energized by the complex I substrates, glutamate/malate (not succinate), Fink et al. showed that free Ca^{2+} at 450 nM enhanced respiration and ATP production, but inhibited these processes at 10 μM or higher concentrations [46].

We observed earlier that MPTP opening in rat liver mitochondria caused ultrastructural disturbances, effective inhibition of respiratory activity, uncoupling respiration and oxidation processes, as well as mitochondrial potential dissipation in the presence of lower concentrations of exogenous Ca^{2+} (20–60 μM) [20, 30] compared to heart mitochondria. The susceptibility of cardiac mitochondria to calcium-induced MPTP opening was much lower, but the susceptibility of mitochondrial respiration was much higher in comparison with liver mitochondria. Similarly, Drahotka and coauthors demonstrated earlier that as compared to liver mitochondria, the MPTP formation in cardiac mitochondria was more resistant to damaging effects of the calcium load and oxidative stress [47].

Conclusions

Our present findings demonstrate numerous effects of exogenously applied calcium on cardiac mitochondria: the low concentrations of Ca^{2+} ions (calculated Ca^{2+} -free concentrations were of 40 to 250 nM) dose-dependently inhibited the succinate-stimulated oxygen consumption rate V_2 and the ADP-dependent oxygen consumption rate V_3 without

significant changes in the coefficients RCR and ADP/O. The high exogenous Ca^{2+} ion concentrations (the free Ca^{2+} concentration was $550 \mu\text{M}$) promoted a dramatic increase in mitochondrial heterogeneity in size and electron density due to the occurrence of swollen organelles with an electron-light matrix, a larger size, an irregular shape, elongation of the intercrisae spaces, and a damaged native structure of the inner membrane of rat heart mitochondria. The ultrastructural disturbances in heart mitochondria were connected with calcium-induced opening of the MPTP and membrane depolarization, observed at free Ca^{2+} concentrations from 150 to $750 \mu\text{M}$. Using the Lineweaver-Burk plot of the dependence of the reciprocal apparent swelling rate ($\text{min}/\Delta\text{D}^{540}$) on the reciprocal Ca^{2+} concentration ($1/[\text{Ca}^{2+}]$), we calculated the apparent Michaelis-Menten constant of Ca^{2+} ion interactions with rat cardiac mitochondria sites, $K_m = 350 \pm 50 \mu\text{M}$. As compared to liver mitochondria, the sensitivity of rat heart mitochondria to Ca^{2+} was much lower in the case of MPTP opening and much higher in the case of respiration inhibition. The preliminary exposure of cardiac mitochondria to the flavonoid naringin alone affected the morphometrical parameters ($200 \mu\text{M}$): increased the average section area and the perimeter of mitochondria, stimulated membrane potential loss ($25\text{--}75 \mu\text{M}$) in the absence of Ca^{2+} , partially prevented Ca^{2+} ion-induced morphological transformations ($200 \mu\text{M}$) in mitochondria, dose-dependently ($25\text{--}75 \mu\text{M}$) diminished the oxygen-consumption rates V_3 and V_2 in the absence or in the presence of Ca^{2+} ions, as well as inhibited Ca^{2+} ion-stimulated MPTP opening. These effects of weak-acidic and lipophilic naringin could be explained due to a direct interaction of naringin with mitochondrial membrane, its protonophoric/ionophoric properties. Our findings suggest that the decrease in membrane potential by naringin diminishes the potential-dependent accumulation of calcium ions by mitochondria.

Supplementary Information The online version contains supplementary material available at <https://doi.org/10.1007/s11010-024-04935-z>.

Acknowledgements This study was partially supported by grant No M23KI – 14 for Joint scientific projects from the Belarusian Republican Foundation for Fundamental Research – National Scientific Foundation of China.

Author contributions T.A. Kavalenia: investigation, data curation, software, E.A. Lapshina: data curation, validation, software, writing-original draft preparation, T.V. Ilyich: investigation, software, visualization, Hu-Cheng Zhao: conceptualization, methodology, supervision, I.B. Zavadnik: conceptualization, writing-reviewing and editing. All the authors approved the final version of the manuscript.

Data availability All the data generated or analyzed during this study have been included in this article.

Declarations

Competing interests The authors declare no competing interests.

Consent to participate All the authors meet the qualifications for authorship and had an opportunity to read and comment on the manuscript. All the authors support publication of the manuscript in Molecular and Cellular Biochemistry.

References

1. Taegtmeier H (1994) Energy metabolism of the heart: from basic concepts to clinical applications. *Curr Probl Cardiol* 19:59–113. [https://doi.org/10.1016/0146-2806\(94\)90008-6](https://doi.org/10.1016/0146-2806(94)90008-6)
2. Bers DM (2001) Excitation-contraction coupling and cardiac contractile force. Springer, Dordrecht
3. Bers DM (2002) Cardiac excitation-contraction coupling. *Nature* 415:198–205. <https://doi.org/10.1038/415198a>
4. Drake KJ, Sidorov VY, McGuinness OP, Wasserman DH, Wikswo JP (2012) Amino acids as metabolic substrates during cardiac ischemia. *Exp Biol Med* 237:1369–1378. <https://doi.org/10.1258/ebm.2012.012025>
5. Yu F, McLean B, Badiwala M, Billia F (2022) Heart failure and drug therapies: a metabolic review. *Int J Mol Sci* 23:2960. <https://doi.org/10.3390/ijms23062960>
6. Williams GSB, Boyman L, Lederer WJ (2015) Mitochondrial calcium and the regulation of metabolism in the heart. *J Mol Cell Cardiol* 78:35–45. <https://doi.org/10.1016/j.yjmcc.2014.10.019>
7. Zhang X, Tomar N, Kandel SM, Audi SH, Cowley AW Jr, Dash RK (2022) Substrate- and calcium-dependent differential regulation of mitochondrial oxidative phosphorylation and energy production in the heart and kidney. *Cells* 11:131. <https://doi.org/10.3390/cells11010131>
8. Carafoli E (2002) Calcium signaling: a tale for all seasons. *Proc Natl Acad Sci USA* 99:1115–1122. <https://doi.org/10.1073/pnas.032427999>
9. Gilbert G, Demydenko K, Dries E, Puertas RD, Jin X, Sipido K, Roderick HL (2020) Calcium signaling in cardiomyocyte function. *Cold Spring Harb Perspect Biol* 12:a035428. <https://doi.org/10.1101/cshperspect.a035428>
10. Garbincius JF, Elrod JW (2022) Mitochondrial calcium exchange in physiology and disease. *Physiol Rev* 102:893–992. <https://doi.org/10.1152/physrev.00041.2020>
11. El Hadi H, Vettor R, Rossato M (2019) Cardiomyocyte mitochondrial dysfunction in diabetes and its contribution in cardiac arrhythmogenesis. *Mitochondrion* 46:6–14. <https://doi.org/10.1016/j.mito.2019.03.005>
12. Bowser DN, Minamikawa T, Nagley P, Williams DA (1998) Role of mitochondria in calcium regulation of spontaneously contracting cardiac muscle cells. *Biophys J* 75:2004–2014. [https://doi.org/10.1016/S0006-3495\(98\)77642-8](https://doi.org/10.1016/S0006-3495(98)77642-8)
13. Kirichok Y, Krapivinsky G, Clapham DE (2004) The mitochondrial calcium uniporter is a highly selective ion channel. *Nature* 427:360–364. <https://doi.org/10.1038/nature02246>
14. Granatiero V, Pacifici M, Raffaello A, De Stefani D, Rizzuto R (2019) Overexpression of mitochondrial calcium uniporter causes neuronal death. *Oxid Med Cell Longev* 2019:1681254. <https://doi.org/10.1155/2019/1681254>
15. Santo-Domingo J, Demarex N (2010) Calcium uptake mechanisms of mitochondria. *Biochim Biophys Acta* 1797:907–912. <https://doi.org/10.1016/j.bbabi.2010.01.005>
16. Knowlton AA, Chen L, Malik ZA (2014) Heart failure and mitochondrial dysfunction: the role of mitochondrial fission/fusion abnormalities and new therapeutic strategies. *J Cardiovasc Pharmacol* 63:196–206. <https://doi.org/10.1097/01.fjc.0000432861.55968.a6>

17. Chistiakov DA, Shkurat TP, Melnichenko AA, Grechko AV, Orekhov AN (2018) The role of mitochondrial dysfunction in cardiovascular disease: a brief review. *Ann Med* 50:121–127. <https://doi.org/10.1080/07853890.2017.1417631>
18. Uryash A, Mijares A, Flores V, Adams JA, Lopez JR (2021) Effects of naringin on cardiomyocytes from a rodent model of type 2 diabetes. *Front Pharmacol* 12:719268. <https://doi.org/10.3389/fphar.2021.719268>
19. Rajadurai M, Stanely Mainzen Prince P (2007) Preventive effect of naringin on cardiac mitochondrial enzymes during isoproterenol-induced myocardial infarction in rats: a transmission electron microscopic study. *J Biochem Mol Toxicol* 21:354–631. <https://doi.org/10.1002/jbt.20203>
20. Zavodnik IB, Kovalenia TA, Veiko AG, Lapshina EA, Ilyich TV, Kravchuk RI, Zavodnik LB, Klimovich II (2022) Structural and functional changes in rat liver mitochondria under calcium ion loading in the absence and presence of flavonoids. *Biomed Khim* 68:237–249. <https://doi.org/10.18097/PBMC20226804237>
21. EGTA - Version 2.0 HTML/JavaScript by PeteSmif. https://pcwww.liv.ac.uk/~petesmif/petesmif/software/_webware06/EGTA/EGTA.htm. Accessed 13 January 2023
22. Guide for the Care and Use of Laboratory Animals. National Research Council US (2011) National Academies Press, Washington. <https://nap.nationalacademies.org/read/12910/chapter/3>. Accessed 13 Jan 2023
23. Johnson D, Lardy HA (1967) Isolation of liver or kidney mitochondria. *Meth Enzymol* 10:94–101
24. Gostimskaya I, Galkin A (2010) Preparation of highly coupled rat heart mitochondria. *J Vis Exp* 23:2202. <https://doi.org/10.3791/2202>
25. Lowry OH, Rosebrough NJ, Farr AL, Randall RJ (1951) Protein measurement with the Folin phenol reagent. *J Biol Chem* 193:265–275. [https://doi.org/10.1016/s0021-9258\(19\)52451-6](https://doi.org/10.1016/s0021-9258(19)52451-6)
26. Millonig GA (1961) Advantages of a phosphate buffer for osmium tetroxide solutions in fixation. *J Appl Physics* 32:1637–1643
27. Reynolds ES (1963) The use of lead citrate at high pH as an electron opaque stain in electron microscopy. *J Cell Biol* 17:208–212. <https://doi.org/10.1083/jcb.17.1.208>
28. Akerman KE, Wikström MK (1976) Safranin as a probe of the mitochondrial membrane potential. *FEBS Lett* 68:191–197. [https://doi.org/10.1016/0014-5793\(76\)80434-6](https://doi.org/10.1016/0014-5793(76)80434-6)
29. Moore AL, Bonner WD (1982) Measurements of membrane potentials in plant mitochondria with the safranin method. *Plant Physiol* 70:1271–1276. <https://doi.org/10.1104/pp.70.5.1271>
30. Golovach NG, Cheshchevik VT, Lapshina EA, Ilyich TV, Zavodnik IB (2017) Calcium-induced mitochondrial permeability transitions: parameters of Ca²⁺ ion interactions with mitochondria and effects of oxidative agents. *J Membr Biol* 250:225–236. <https://doi.org/10.1007/s00232-017-9953-2>
31. Miyamae M, Camacho SA, Weiner MW, Figueredo VM (1996) Attenuation of postischemic reperfusion injury is related to prevention of [Ca²⁺]_m overload in rat hearts. *Am J Physiol* 271:H2145–H2153. <https://doi.org/10.1152/ajpheart.1996.271.5.H2145>
32. Rosca MG, Vazquez EJ, Kerner J, Parland W, Chandler MP, Stanley W, Sabbah HN, Hoppel CL (2008) Cardiac mitochondria in heart failure: decrease in respirasomes and oxidative phosphorylation. *Cardiovasc Res* 80:30–39. <https://doi.org/10.1093/cvr/cvn184>
33. Hollander JM, Thapa D, Shepherd DL (2014) Physiological and structural differences in spatially distinct subpopulations of cardiac mitochondria: influence of cardiac pathologies. *Am J Physiol Heart Circ Physiol* 307:H1–H14. <https://doi.org/10.1152/ajpheart.00747.2013>
34. Shimada T, Horita K, Murakami M, Ogura R (1984) Morphological studies of different mitochondrial populations in monkey myocardial cells. *Cell Tissue Res* 238:577–582. <https://doi.org/10.1007/BF00219874>
35. Sandoval-Acuña C, Ferreira J, Speisky H (2014) Polyphenols and mitochondria: an update on their increasingly emerging ROS-scavenging independent actions. *Arch Biochem Biophys* 559:75–90. <https://doi.org/10.1016/j.abb.2014.05.017>
36. Veiko AG, Sekowski S, Lapshina EA, Wilczewska AZ, Markiewicz KH, Zamarava M, Zhao Hu-cheng, Zavodnik IB (2020) Flavonoids modulate liposomal membrane structure, regulate mitochondrial membrane permeability and prevent erythrocyte oxidative damage. *Biochim Biophys Acta* 1862:183442. <https://doi.org/10.1016/j.bbame.2020.183442>
37. Cherrak SA, Mokhtari-Soulimane N, Berroukeche F, Bensenane B, Cherbonnel A, Merzouk H, Elhabiri M (2016) *In vitro* antioxidant versus metal ion chelating properties of flavonoids: a structure-activity investigation. *PLoS ONE* 11:e0165575. <https://doi.org/10.1371/journal.pone.0165575>
38. Ortega R, García N (2009) The flavonoid quercetin induces changes in mitochondrial permeability by inhibiting adenine nucleotide translocase. *J Bioenerg Biomembr* 41:41–47. <https://doi.org/10.1007/s10863-009-9198-6>
39. De Marchi U, Biasutto L, Garbisa S, Toninello A, Zoratti M (2009) Quercetin can act either as an inhibitor or an inducer of the mitochondrial permeability transition pore: a demonstration of the ambivalent redox character of polyphenols. *Biochim Biophys Acta* 1787:1425–1432. <https://doi.org/10.1016/j.bbabi.2009.06.002>
40. Lemasters JJ, Theruvath TP, Zhong Z, Nieminen A-L (2009) Mitochondrial calcium and the permeability transition in cell death. *Biochim Biophys Acta* 1787:1395–1401. <https://doi.org/10.1016/j.bbabi.2009.06.009>
41. Neginskaya MA, Morris SE, Pavlov EV (2022) Both ANT and ATPase are essential for mitochondrial permeability transition but not depolarization. *iScience* 25(11):105447. <https://doi.org/10.1016/j.isci.2022.105447>
42. Williams GSB, Boyman L, Chikando AC, Khairallah RJ, Lederer WJ (2013) Mitochondrial calcium uptake. *Proc Natl Acad Sci USA* 110:10479–10486. <https://doi.org/10.1073/pnas.1300410110>
43. Bernardi P (2020) Mechanisms for Ca²⁺-dependent permeability transition in mitochondria. *Proc Natl Acad Sci USA* 117:2743–2744. <https://doi.org/10.1073/pnas.1921035117>
44. Halestrap AP, Pasdois P (2009) The role of the mitochondrial permeability transition pore in heart disease. *Biochim Biophys Acta* 1787:1402–1415. <https://doi.org/10.1016/j.bbabi.2008.12.017>
45. Anmann T, Eimre M, Kuznetsov AV, Andrienko T, Kaambre T, Sikk P, Seppet E, Tiivel T, Vendelin M, Seppet E, Saks VA (2005) Calcium-induced contraction of sarcomeres changes the regulation of mitochondrial respiration in permeabilized cardiac cells. *FEBS J* 272:3145–3161. <https://doi.org/10.1111/j.1742-4658.2005.04734.x>
46. Fink BD, Bai F, Yu L, Sivitz WI (2017) Regulation of ATP production: dependence on calcium concentration and respiratory state. *Am J Physiol Cell Physiol* 313:C146–C153. <https://doi.org/10.1152/ajpcell.00086.2017>
47. Drahota Z, Milerová M, Endlicher R, Rychtmoc D, Červinková Z, Ošťádal B (2012) Developmental changes of the sensitivity of cardiac and liver mitochondrial permeability transition pore to calcium load and oxidative stress. *Physiol Res* 61:S165–S172. <https://doi.org/10.33549/physiolres.932377>

Publisher's Note Springer Nature remains neutral with regard to jurisdictional claims in published maps and institutional affiliations.

Springer Nature or its licensor (e.g. a society or other partner) holds exclusive rights to this article under a publishing agreement with the author(s) or other rightsholder(s); author self-archiving of the accepted manuscript version of this article is solely governed by the terms of such publishing agreement and applicable law.